Thermochimica Acta 498 (2010) 54–60

Contents lists available at ScienceDirect

Thermochimica Acta

journal homepage: www.elsevier.com/locate/tca

Dissolving behavior and calcium release from fibrous wollastonite in acetic acid solution

Petr Ptáček*, Magdaléna Nosková, Jiří Brandštetr, František Šoukal, Tomáš Opravil

Institute of Materials Science, Faculty of Chemistry, Brno University of Technology, Purkyňova 464/118, Brno CZ-621 00, Czech Republic

ARTICLE INFO

Article history:
Received 29 May 2009
Received in revised form 2 October 2009
Accepted 5 October 2009
Available online 13 October 2009

Keywords:
Wollastonite
Calcium silicate
Silica
Acetic acid
Dissolution of silicates
Carbon dioxide sequestration

ABSTRACT

The degradability of fibrous wollastonite ($CaSiO_3$) in an aqueous solution of acetic acid and leaching of Ca^{2+} ions were investigated in the temperature range from 22 to 50 °C. The Inductively Coupled Plasma Atomic Emission Spectroscopy (ICP-OES) was used for the assessment of calcium and other selected cations in the leaching medium. The amount of calcium in the solvent can be significantly enhanced through leaching at higher temperature. Fibrous silica particles are the main by-product of the leaching process. The properties of by-product were examined by thermal analysis (simultaneous TG–DTA–EGA), infrared spectroscopy (FT-IR) and scanning electron microscopy (SEM). The formation of silica layer on the surface of fibrous wollastonite particles is an important factor in the leaching process. Particles were covered by the silica layer and wollastonite core size was continually decreasing during leaching. The shape of resulting silica particles shows no significant changes during this process. Specific surface of the formed fibrous silica particles strongly depends on the leaching temperature.

1. Introduction

The 20th century has been experiencing the rapid increase of population and huge growth in energy consumption. As more countries become industrialized, it is expected that more energy will be consumed in the 21st century. Fossil fuels have been the world's primary source of energy for well over a century. They currently account for nearly 85% of world's energy supply. This trend is expected to continue throughout the 21st century [1,2].

The increasing carbon dioxide content in the atmosphere and its long-term effect on the climate has led to increasing interest and research on the possibilities of capture, utilization and long-term storage of CO_2. One of the major options for reduction of anthropogenic CO_2 emissions in the near future is the carbon dioxide capture and storage (CCS) technologies. This concept includes capture (separation and compression) of CO_2 from large centralized CO_2 emitters (such as power plants, metallurgy and cement producers), and transportation to an adequate storage site (such as depleted oil and gas fields or saline aquifers). Carbonation of natural silicate minerals and fixing of carbon dioxide as carbonates is an interesting alternative option for long-term storage of CO_2 because suitable calcium and magnesium rich rocks are distributed all over the world. Carbonation of calcium and magnesium silicates, such as wollastonite ($CaSiO_3$), enstatite ($MgSiO_3$), olivine (Mg_2SiO_4) and many other minerals, traps CO_2 as environmentally stable solid carbonates that could provide considerable storage capacity within a geological time scale. The silicate rock could be turned into environmentally stable carbonates by following mechanism [1–8]:

$$(Ca, Mg)_xSi_yO_{x+2y} + xCO_2 \rightarrow x(Ca, Mg)CO_3 + ySiO_2. \quad (1)$$

The proposal to remove greenhouse gases by pumping liquefied CO_2 several kilometers under the ground (geosequestration) implies that many carbonate minerals will be formed. Among these minerals brugnatellite and coalingite with the hydrotalcite structure are probable. The study of the magnesium carbonates is of importance in the development of technology for the removal of greenhouse gases [9–11]. For wollastonite, overall carbonation process can be written as [8,12,13]:

$$CaSiO_3 + CO_2 \rightarrow CaCO_3 + SiO_2. \quad (2)$$

Industrial residues, such as steel slag and municipal solid waste incinerator bottom ash, are promising materials for mineral carbonation too [3,8,14–17].

The most efficient processes suggested for carbonation involve leaching or dissolution of calcium or magnesium silicates in liquid media and precipitation of carbonates or hydroxides during subsequent carbonation. The process consists of two main steps. The first one, calcium or magnesium ions are extracted from natural silicates by leaching with acetic acid [3,7]:

$$CaSiO_3 + 2CH_3CO_2H \rightarrow Ca^{2+} + 2CH_3CO_2^- + SiO_2 + H_2O; \quad (3)$$

$$MgSiO_3 + 2CH_3CO_2H \rightarrow Mg^{2+} + 2CH_3CO_2^- + SiO_2 + H_2O. \quad (4)$$

* Corresponding author. Tel.: +420 541 149 389; fax: +420 541 149 361.
E-mail address: ptacek@fch.vutbr.cz (P. Ptáček).

0040-6031/$ – see front matter © 2009 Elsevier B.V. All rights reserved.
doi:10.1016/j.tca.2009.10.002

Table 1
Properties and results of the chemical analysis of wollastonite.

Specific humidity	Ignition loss	Calcite[a]	Sample composition (%)[b]					
			Ca	Al	Fe	Ni	Zn	SiO_2[c]
0.13%	2.36%	5.57%	32.30	0.24	0.17	0.07	0.08	49.18

[a] Admixture quantity was calculated from TGA results (please see Fig. 5).
[b] The sample was fused with Na_2CO_3 in Pt crucible and melt was leached out by diluted HCl. The precipitated silica was filtered out and composition of the filtrate was analyzed by ICP-OES. Collected data were corrected to results of reference sample. Alkaline fusion was used due to assumed content of aluminosilicates in the sample.
[c] Amount of precipitated SiO_2 was determined by gravimetric analysis.

The behavior of some other fibrous silicates, such as amosite, crocidolite, chrysotile, sepiolite, palygorskite, in acid media has been reported [18–20]. After filtrating silica out of the solution, carbon dioxide is pumped into the solution, forming calcium or magnesium carbonates that precipitate from the solution:

$$Ca^{2+} + 2CH_3CO_2^- + CO_2 + H_2O \rightarrow CaCO_3 + 2CH_3CO_2H; \quad (5)$$

$$Mg^{2+} + 2CH_3CO_2^- + CO_2 + H_2O \rightarrow MgCO_3 + 2CH_3CO_2H. \quad (6)$$

Acetic acid is recovered in this step and recycled for use in the next extraction step [3,7]. Most of these processes have been considered to be too expensive for CO_2 storage, since they require energy for crushing, grinding or preheating and possible chemical additives which cannot be recovered. However, published experimental data on these processes are scarce and occasionally contradictory [7].

The present paper is aimed at the study of leaching process of calcium from wollastonite in the aqueous solution of acetic acid. The effect of temperature on the amount of extracted calcium and properties of residual fibrous silica particles was evaluated by thermal analysis, infrared spectroscopy and BET. Specific surface area of silica by-products is very important property for its potential application. Research on exploitation of residual silica is required due to its large contents in minerals which are supposed for mineral carbonation process. A paper dealing with the kinetics of leaching process is being prepared.

2. Experimental procedure

The wollastonite obtained from Ankerpoort NV: The Mineral Company (Netherlands), with specific surface area of 0.66 $m^2\,g^{-1}$ (Chembet 3000) was used in this study. The 90 μm undersize particles of sample were employed without other treatment. According to X-ray crystallography results (Siemens D500) the calcite, quartz and small amount of mica or chlorite group minerals are accessory minerals of wollastonite. Some properties and composition of applied wollastonite are listed in Table 1.

Dissolution experiments were carried out on stirred suspension of wollastonite in aqueous solution of acetic acid (Lachema, p.a.). Temperature of leaching bath ranged from 22 to 50 °C. The temperature of double wall glass reactor was adjusted using external water flow of temperature controlled water batch (thermostat). Sample was poured on by solution of acetic acid that was preheated to the applied leaching temperature in water batch of thermostat. The stability of suspension is very poor due to low value of electrokinetic (zeta) potential that is only −19.7 mV (Zeta meter Brookhaven 90 Plus). Hence, the stirring of system by magnetic stirrer was used. Suspension contained 12.5 g of wollastonite per liter of leaching solution with concentration of acetic acid of about 3 mol dm^{-3}. The pH value of dispersing medium for 24 h leaching experiment was continuously measured by pH meter connected to PC.

Solid part of suspension was separated by filtration through dense filter paper (red strip) after leaching. Filter cake was washed three times by slightly acidified (acetic acid) distilled water. The quantities of ions in original sample and leachate were determined by the Inductively Coupled Plasma Atomic Emission Spectroscopy (ICP-OES; ICP IRIS Iterdip II XSP duo). Filter cake was dried at 110 °C, its properties and composition were subsequently investigated by simultaneous TG–DTA–EGA, FT-IR, BET and SEM.

Thermal analyses (simultaneous TG–DTA) were made with TG–DTA analyzer TA Instruments Q600 connected to heated gas cell of FT-IR spectrometer Thermo Nicolet iS10 via heated capillary due to investigation of gases releasing from the sample (EGA). All methods were carried out at the same time on one sample heated up at rate of 20 °C min^{-1} under flow of argon (100 $cm^3\,min^{-1}$).

Infrared spectra were collected with FT-IR spectrometer Thermo Nicolet iS10 via KBr pellets technique. Specimens were ground with dried spectroscopic grade KBr powder and the mixture was compressed to pellets for FT-IR measurements. The sample to KBr mass ratio was 1:100. All spectra are collected in the 4000–400 cm^{-1} range at 8 cm^{-1} resolution.

3. Results and discussion

3.1. Leaching test

The typical time dependence of pH is shown in Fig. 1. The pH of leaching medium increased during dissolution of wollastonite. Nevertheless, when the solution of acetic acid was introduced into the reactor, the fast dissolution of calcite began and next the pH value stayed almost constant during a short induction period (see details in Fig. 1). The reaction began probably immediately after wetting process, but the amount of dissolved material remained very small for a certain time. The induction period is not rare phenomenon for heterogeneous processes. Some authors explain this delay at the beginning of the process by the nucleation incubation period, i.e. such as the transient time in which the steady rate of formation of nuclei is reached [21–23]. Other published explanations of induction period depend on the chemistry of dissolution process or crystal lattice stability [24–27]. Our experiments show that induction period takes a longer time in case of lower temperatures and lower acid concentrations.

The buffer system of weak acid (CH_3CO_2H) and its salt ($Ca(CH_3CO_2)_2$) with a strong base, i.e. $Ca(OH)_2$, was formed dur-

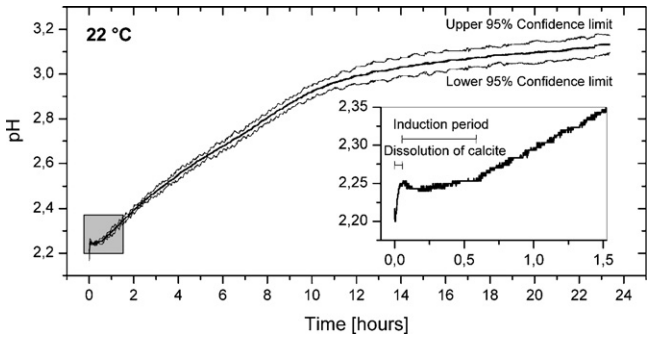

Fig. 1. Dissolution of wollastonite in acetic acid at 22 °C including the induction period.

Table 2
The temperature dependence of calcium and some other elements leaching efficiency per gram of wollastonite raw material after 24 h. Significant values of Pearson correlation coefficient (R) are typed by bold.

Element		Temperature (°C)							
		22	25	30	35	40	45	50	R
Ca	P (%)	67.6	72.1	79.0	84.7	89.4	93.6	94.4	**0.986**
Al		0.4	0.4	0.3	0.2	0.2	0.3	0.2	**−0.772**
Fe		9.8	11.3	13.5	16.0	17.4	19.7	21.6	**0.998**
Ni		2.4	2.7	3.4	4.7	4.5	5.3	5.9	**0.982**
Zn		18.3	29.1	3.9	13.5	10.3	16.3	12.4	−0.363

ing dissolution of wollastonite (Eq. (3)). With respect to reaction stoichiometry, the amount of formed acetate ions was double the concentration of Ca^{2+} ions released from wollastonite. Therefore following subform of Henderson buffer equation may be used for estimation of the course of leaching process:

$$\mathrm{pH}(T) = p\mathrm{K_a}(T) + \log\frac{2[\mathrm{Ca^{2+}}]}{[\mathrm{CH_3CO_2H}]} \quad (7)$$

Nevertheless, the measured data must be corrected to Ca^{2+} ions released during dissolution of calcite before Eq. (7) can be applied to dissolution of wollastonite.

It is evident that the course of wollastonite dissolution and leaching of calcium through the formed silica layer can be monitored via pH of system, because the content of calcium is much higher than the amount of other ions, which can be released from wollastonite (see Table 1). Naturally there must be sufficient excess of acetic acid in the reaction mixture so that its concentration is practically constant during the leaching process.

Filtrates gained from 24 h lasting dissolution of wollastonite in the aqueous solution of acetic acid within temperature range from 22 to 50 °C were analyzed by ICP-OES to determine the concentrations of calcium and some other relevant elements, such as Fe, Ni and Zn. The leaching efficiency (P) can be evaluated as a mass ratio of element extracted from unit weight of wollastonite to the amount of this component in the original sample. Table 2 shows the results.

Acquired data confirm that the amount of extracted calcium is markedly increasing with growing temperature of leaching batch. The amount of extracted calcium has increased up to about 27% within the investigated temperature interval. Moreover, a significant linear relationship between temperature and quantity of calcium was found using correlation analysis. The effect of temperature on leaching efficiency of calcium is shown in Fig. 2. It must be pointed out that only simple extrapolation to 100% efficiency provides incorrect value due to other ions present in the wollastonite structure, admixtures of other minerals in the sample as well as in consequences of adsorption events.

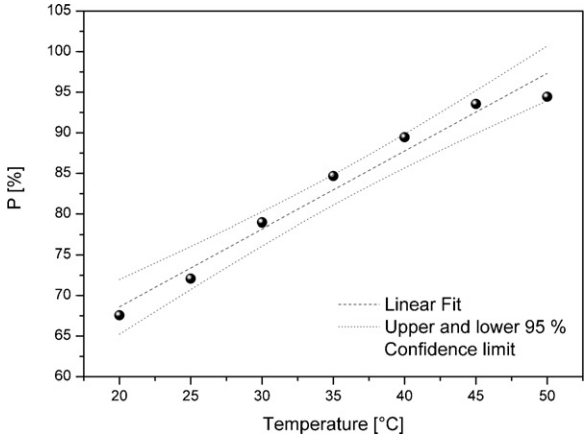

Fig. 2. The effect of temperature on the leaching efficiency of calcium from wollastonite raw material.

Calcium is not the only element among elements noted in Table 2 which shows linear temperature dependence of concentration. The Fe and Ni contents in leaching medium were increasing with increasing leaching temperature. Acceleration of diffusion phenomenon with increasing temperature gives the reason for this fact. Furthermore, according to correlation analysis results, the amount of calcium correlates with quantities of Fe and Ni. That implies that lattice of utilized wollastonite may contain cations of these elements.

Silica or more exactly mainly silica containing gel phase was formed during dissolution of wollastonite in acetic acid (Eq. (3)). The mass of original sample was reduced to 58 ± 2% during this process. Hence besides the application of leaching process in CCS technology the problem of by-products utilization must be solved as well. In other words proper exploitation of by-product is an integral part of leaching technology.

The specific surface area is one of the most important parameter for potential application of by-products, for example such as adsorbent, carrier of catalysts or reactive admixture in concrete technology. The influence of temperature on specific surface area of nascent SiO_2 xerogel is presented in Table 3. Acquired data show that specific surface area is strongly influenced by temperature. Over studied temperature range from 22 to 50 °C the specific surface area increased from 73 to 146 $m^2\,g^{-1}$, i.e. its value grew approximately twice. Furthermore, the significant statistical correlation has been found between temperature of leaching bath and specific surface area.

The fact must be pointed out that behavior of silica based dispersion systems can be influenced by many factors (temperature, pH, presence of salt, concentration, etc.). This area of colloidal chemistry was described in details by Iler [28].

3.2. Infrared spectroscopy

The infrared spectrum of wollastonite is given in Fig. 3. The peaks at 1081, 1060, 1016, 965, 925, 900, 682, 643, 568, 472 and 451 cm^{-1} belong to β-$CaSiO_3$ [29]. The high-wavenumber band at 1250–800 cm^{-1}, mid-wavenumber band at 800–600 cm^{-1} and low-wavenumber band 600–400 cm^{-1} were assigned to antisymmetric (ν_3), symmetric (ν_1) and bending mode (ν_4) of the silicate tetrahedron vibrations, respectively [30].

The water adsorbed onto the surface of sample shows a broad stretching band (ν_1) and weak deformation band (ν_2) at 3435 and 1626 cm^{-1}, respectively [9,10,31]. The bands located at 2512, 1798, 1431 and 920 cm^{-1} indicate that $CaCO_3$ is the only sig-

Table 3
Effect of temperature on the specific surface of silica xerogel remaining after dissolution of wollastonite and value of the correlation coefficient (R) between temperature and specific surface of the sample.

T (°C)	22	25	30	35	40	45	50	R
S_{spec} ($m^2\,g^{-1}$)	73	77	102	96	96	133	146	0.927

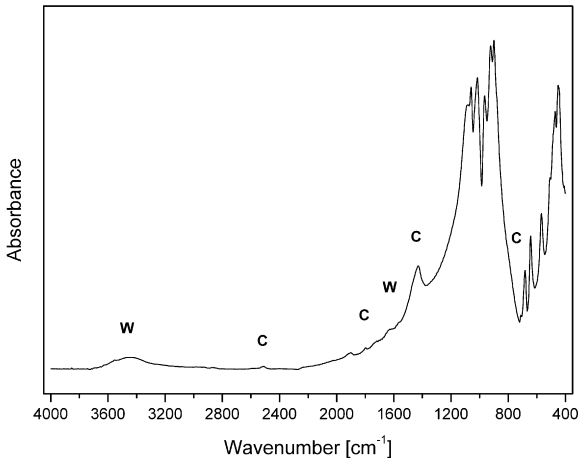

Fig. 3. The baseline corrected FT-IR spectrum of wollastonite. Admixtures bands are designated as following: Calcite, C and adsorbed water, W.

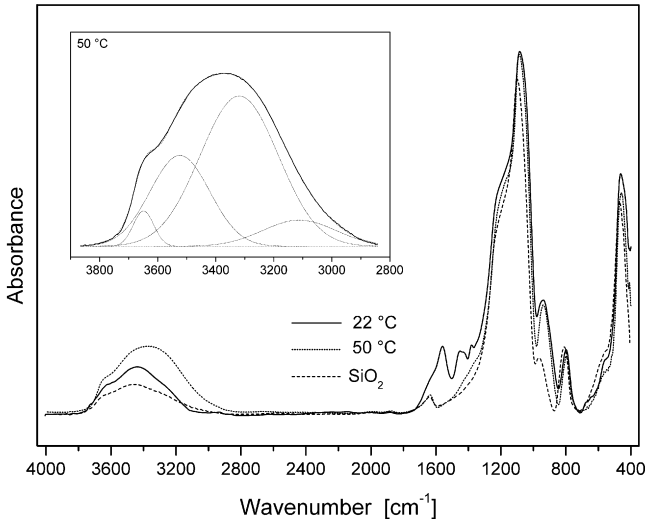

Fig. 4. The baseline corrected FT-IR spectrum of silica based xerogel.

nificant impurity of wollastonite. These bands are assigned as $2\nu_2 + \nu_4$ combination mode, $\nu_1 + \nu_4$ combination mode, antisymmetric stretching (ν_3) and out-of-plane bending (ν_2) of CO_3^{2-} anion, respectively. The absence of symmetric stretching (ν_1) band in infrared spectrum identifies the $CaCO_3$ as calcite [9,10,32].

Fig. 4 shows typical infrared spectra of silica based by-products formed during dissolution of wollastonite at 22 and 50 °C. The higher specific surface area of silica gives the reason for growing intensities of bands at 3451 and 1632 cm^{-1} belonging to water adsorbed onto the surface. The OH vibration region was fitted by Gauss function (see details in Fig. 4). Stretching of free and bonded surface hydroxyl groups at 3647 and 3521 cm^{-1} participate on the structure of band [33]. Bending of silanol groups (SiO–H) is located at 940 cm^{-1} [31].

Two most intensive bands at 1095 and 463 cm^{-1} are attributed to antisymmetric stretching (ν_3) and bending (ν_4) vibration of Si–O bond in the SiO_4 tetrahedron, respectively. The Si–O symmetric stretching vibration (ν_1) is located at 805 cm^{-1} [31,34]. It explains the reason that silica is the main part of sample after leaching process. Other bands belong to residual wollastonite and remaining acetic acid adsorbed on the silica surface.

The spectrum of pure SiO_2 is also plotted in Fig. 4. The comparison of all spectra leads to conclusion that certain amount of wollastonite is still present after leaching at 22 °C, whereas the sample after leaching at 50 °C consists of silica only.

3.3. Simultaneous TG–DTA–EGA

Thermal analysis of wollastonite is given in Fig. 5. The total mass loss of the sample over whole analyzed temperature interval (25–1250 °C) is 2.80%. Wollastonite undergoes the phase transition of low-temperature wollastonite (β-$CaSiO_3$) to high-temperature phase (α-$CaSiO_3$) at 1125 °C. Therefore, any effects on the thermal curves and infrared spectra of evolved gases belong to impurities.

The weak endothermic DTA peak with maximum at 98 °C is due to the loss of water molecules. The experimentally determined mass loss for this peak is 0.07%. The two following inexpressive endotherms at 207 and 374 °C appeared probably due to presence of chlorite or mica group admixtures in the sample. Dehydration and dehydroxylation are connected with mass loss of about 0.10 and 0.04% on TG curve. Thermal decomposition of $CaCO_3$ at 710 °C is the most expressive process in Fig. 5. The observed mass loss of sample is 2.45%. Calcination of calcite (identified by infrared spectroscopy) is distinctly visible in the EGA pattern.

Silica xerogel was formed during drying step with a total mass loss of 2–4% over the temperature range from 25 to 180 °C (Fig. 6). Endothermic peak at 112 °C corresponds to the elimination of water from silica gel, which is formed during leaching of calcium from wollastonite. Chemisorbed water, i.e. various kinds of silanol groups (≡Si–OH) on the surface of silica, is disappearing over wide temperature interval. The EGA results show that bands of formed water can be recognized almost to 1000 °C.

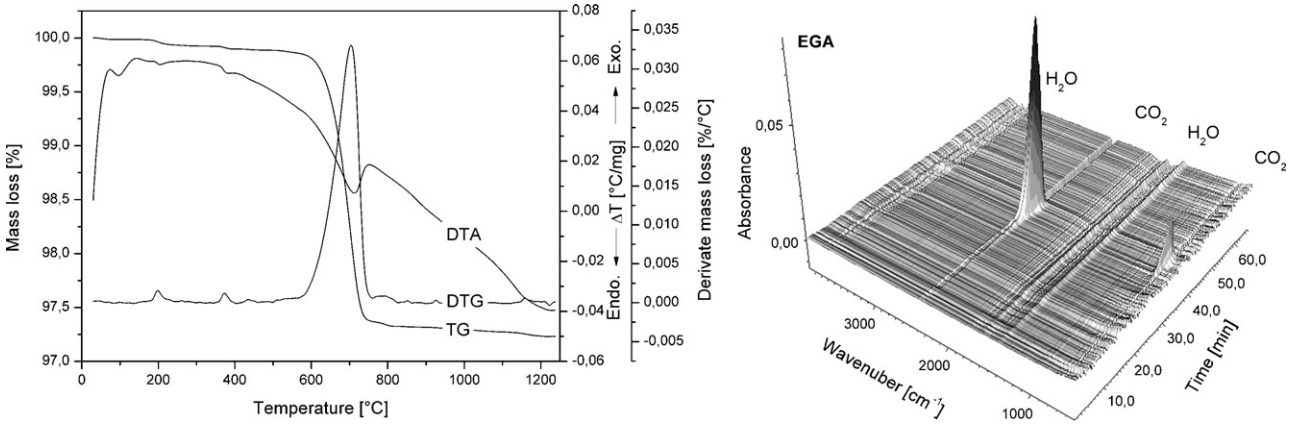

Fig. 5. TG–DTA and EGA of wollastonite.

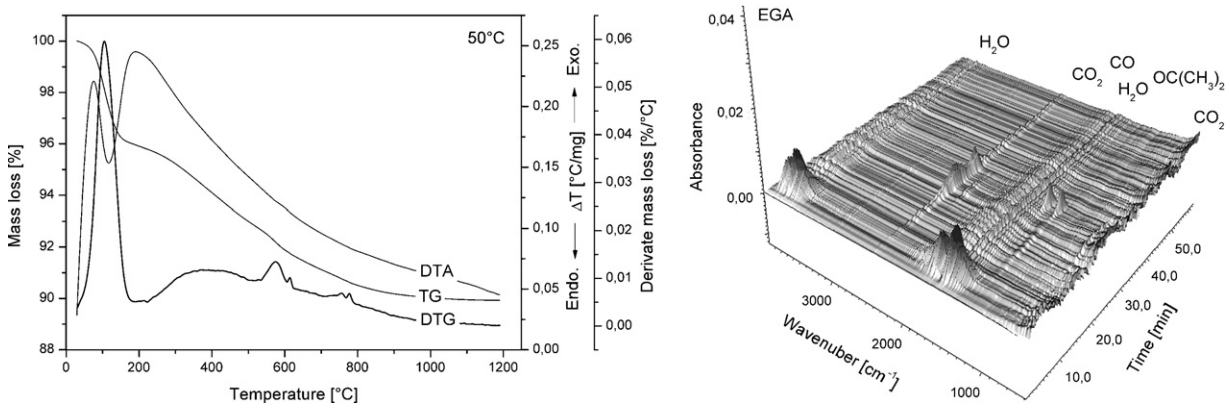

Fig. 6. The typical TG–DTA and EGA plot for by-product of leaching process.

The porous structure of xerogel contains a certain amount of residual calcium acetate monohydrate. The thermal decomposition of $Ca(CH_3COO)_2{\cdot}H_2O$ is divided into four steps: two-stage dehydration (75 and 120 °C), formation of $CaCO_3$ (392 °C) and its calcination to CaO (595 °C) [35]. Hence it proves that dehydration participates on the mass loss of sample during drying step. The pyrolysis of residual amount of calcium acetate begins at 225 °C. The CO_2 and weak CO bands are visible from EGA. Carbon monoxide implies reducing condition and formation of calcite according to Eq. (8). Produced calcite is subsequently calcinated (Eq. (9)) and further CO_2 appears in EGA:

$$Ca(CH_3COO)_2 \rightarrow CaCO_3 + 1.5H_2O \quad (8)$$

$$CaCO_3 \rightarrow CaO + CO_2 \quad (9)$$

The EGA peaks 1337 and 1185 cm^{-1} show that acetone is being formed within the temperature interval ranging from 535 to 620 °C. Studies concerned to thermal decomposition of acetates describe several possible routes of this process where CH_3COCH_3 was formed [36–39]. The mass of sample was reduced for about 5.9% during all these processes.

3.4. Electron scanning microscopy

Microphotographs of wollastonite grains before leaching of calcium are in Fig. 7a. The sample consists of fibrous fine grain forms. The surface of particles shows splinters and uneven fractures. Any other shapes of aggregates belong to admixtures. Some of them show clearly layered structure. That corresponds to thermal analy-

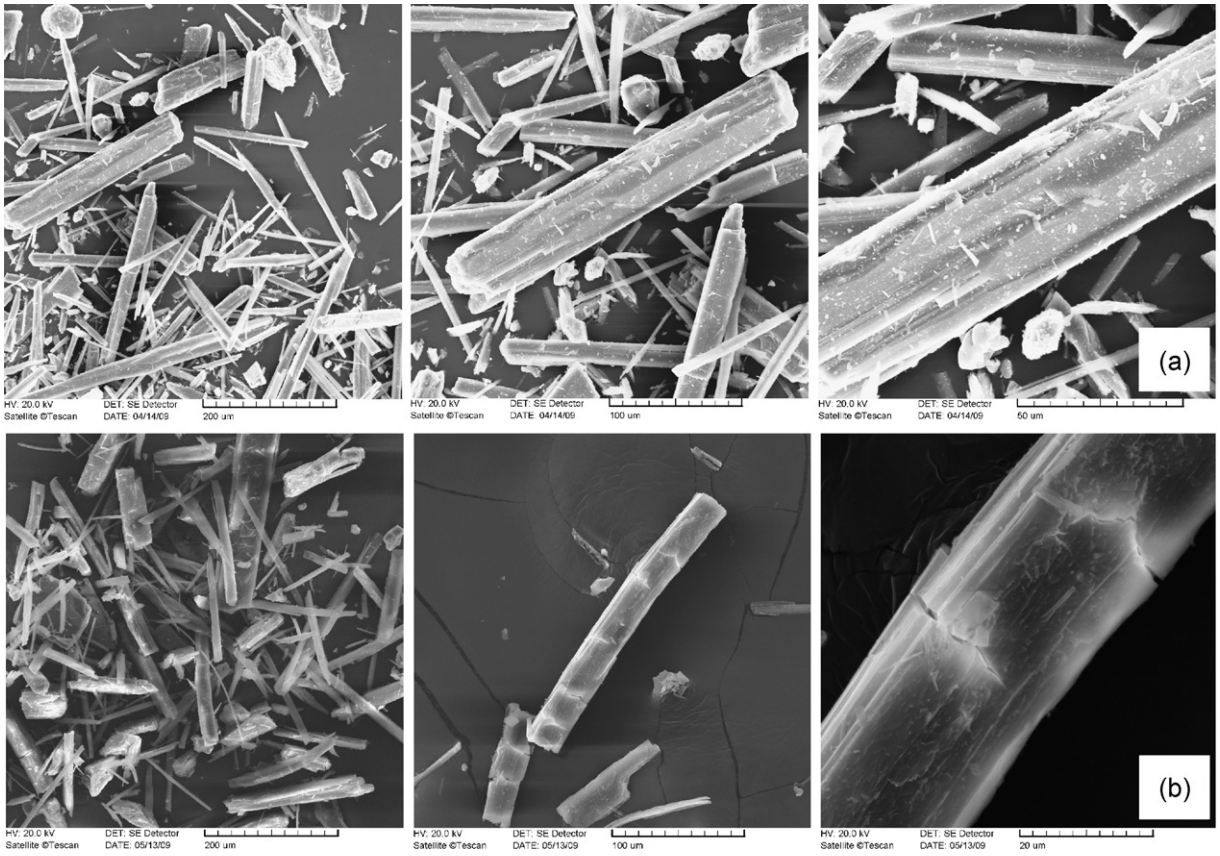

Fig. 7. SEM pictures of fibrous wollastonite particles before (a) and after (b) leaching of calcium. Some of admixtures show layered structure.

sis and FT-IR results, because these methods indicate the presence of phyllosilicates as well.

Typical SEM picture of leaching products is shown in Fig. 7b. Leaching product consists of slightly bent and cracked fibrous particles of silica or silica coated wollastonite core. The cracks of particles probably took place during drying of filter cake due to drying forces leading to shrinkage of the sample. The surface of particles is very different from the wollastonite one. There is not any fine detritus placed on the surface that is much smoother.

These observations show that the shape of particles is preserved during leaching process. The SiO_2 gel layer increased while wollastonite core was gradually disappearing, i.e. there is a topotactical relationship to the parent wollastonite particle. The sizable deformation was observed for sample prepared at higher temperatures. The reason can be found within the absence of the wollastonite core. Thus the behavior during dissolution can be utilized for the preparation of fibrous silica particles with wollastonite core.

4. Conclusion

All tests show that acetic acid is able to extract a significant amount of calcium from wollastonite and that efficiency of the process can be improved through higher temperature of leaching. Dissolution of wollastonite in the aqueous solution of acetic acid is a steady process. The continuous silica layer formed on the surface of wollastonite particles during leaching. Thickness of this layer increased during leaching, while wollastonite core was gradually disappearing. That led to the silica particles with similar shape like original particles of the wollastonite.

The temperature has a significant effect on the dissolution of wollastonite in acetic acid. Furthermore, temperature of the system is an important factor determining the specific surface area of resulting silica xerogel. The system shows huge specific surface area that increases with the higher temperature of leaching. The specific surface area of SiO_2 is one of the most important properties for its potential utilizations, e.g. as an adsorbent, carrier of catalysts, filler or reactive admixture to Portland cement or geopolymers.

There is also another important possibility resulting from the course of dissolution. It is concerned to preparation of fibrous particular composite consisting of wollastonite core and silica shell with a huge, reactive surface. These particles are formed during leaching process at the lower temperatures. The properties of surface silica layer may be controlled by temperature, time and other factors, such as concentration of acid and intensity of stirring during dissolution process.

Acknowledgment

Presented work has been partially supported by project of Ministry of Education, Youth and Sports #2B08024.

References

[1] H. Yang, Z. Xu, M. Fan, R. Gupta, R.B. Slimane, A.E. Bland, I. Wright, Progress in carbon dioxide separation and capture: a review, Journal of Environmental Sciences 20 (2008) 14–27.
[2] M.M. Maroto-Valer, D.J. Fauth, M.E. Kuchta, Y. Zhang, J.M. Andrésen, Activation of magnesium rich minerals as carbonation feedstock materials for CO_2 sequestration, Fuel Processing Technology 86 (2005) 1627–1645.
[3] S. Teir, S. Eloneva, C.-J. Fogelholm, R. Zevenhoven, Dissolution of steelmaking slags in acetic acid for precipitated calcium carbonate production, Energy 32 (2007) 528–539.
[4] K.S. Lackner, C.H. Wendt, D.P. Butt, E.L. Joyce Jr., D.H. Sharp, Carbon dioxide disposal in carbonate minerals, Energy 20 (1995) 1153–1170.
[5] S. Teir, S. Eloneva, C.-J. Fogelholm, R. Zevenhoven, Fixation of carbon dioxide by producing hydromagnesite from serpentinite, Applied Energy 86 (2009) 214–218.
[6] J. Fagerlund, S. Teir, E. Nduagu, R. Zevenhoven, Carbonation of magnesium silicate mineral using a pressurised gas/solid process, Energy Procedia 1 (2009) 4907–4914.
[7] S. Teir, H. Revitzer, S. Eloneva, C.-J. Fogelholm, R. Zevenhoven, Dissolution of natural serpentinite in mineral and organic acids, International Journal of Mineral Processing 83 (2007) 36–46.
[8] W.J.J. Huijgen, R.N.J. Comans, G.-J. Witkamp, Cost evaluation of CO_2 sequestration by aqueous mineral carbonation, Energy Conversion and Management 48 (2007) 1923–1935.
[9] R.L. Frost, B.J. Reddy, S. Bahfenne, J. Graham, Mid-infrared and near-infrared spectroscopic study of selected magnesium carbonate minerals containing ferric iron—implications for the geosequestration of greenhouse gases, Spectrochimica Acta Part A: Molecular and Biomolecular Spectroscopy 72 (2009) 597–604.
[10] R.L. Frost, S. Bahfenne, J. Graham, Infrared and infrared emission spectroscopic study of selected magnesium carbonate minerals containing ferric iron—implications for the geosequestration of greenhouse gases, Spectrochimica Acta Part A: Molecular and Biomolecular Spectroscopy 71 (2008) 1610–1616.
[11] R.L. Frost, S. Bahfenne, J. Graham, W.N. Martens, Thermal stability of artinite, dypingite and brugnatellite—Implications for the geosequestration of greenhouse gases, Thermochimica Acta 475 (2008) 39–43.
[12] W.J.J. Huijgen, G.-J. Witkamp, R.N.J. Comans, Mechanisms of aqueous wollastonite carbonation as a possible CO_2 sequestration process, Chemical Engineering Science 61 (2006) 4221–4242.
[13] T. Kojima, A. Nagamine, N. Ueno, S. Uemiya, Absorption and fixation of carbon dioxide by rock weathering, Energy Conversion and Management 38 (1997) S461–S466.
[14] D.N. Huntzinger, J.S. Gierke, L.L. Sutter, S.K. Kawatra, T.C. Eisele, Mineral carbonation for carbon sequestration in cement kiln dust from waste piles, Journal of Hazardous Materials 168 (2009) 31–37.
[15] G. Montes-Hernandez, R. Pérez-López, F. Renard, J.M. Nieto, L. Charlet, Mineral sequestration of CO_2 by aqueous carbonation of coal combustion fly-ash, Journal of Hazardous Materials 161 (2009) 1347–1354.
[16] R. Baciocchi, G. Costa, A. Polettini, R. Pomi, Influence of particle size on the carbonation of stainless steel slag for CO_2 storage, Energy Procedia 1 (2009) 4859–4866.
[17] Q. Chen, D.C. Johnson, L. Zhu, M. Yuan, C.D. Hills, Accelerated carbonation and leaching behavior of the slag from iron and steel making industry, Journal of University of Science and Technology Beijing, Mineral, Metallurgy, Material 14 (2007) 297–301.
[18] M.P. Allen, R.W. Smit, Dissolution of fibrous silicates in acid and buffered salt solutions, Minerals Engineering 7 (1994) 1527–1537.
[19] L.G. Hernández, L.I. Rueda, A.R. Díaz, C.Ch. Antón, Preparation of amorphous silica by acid dissolution of sepiolite: kinetic and textural study, Journal of Colloid and Interface Science 109 (1986) 150–160.
[20] M.S. Barrios, L.V.F. González, M.A.V. Rodríguez, J.M.M. Pozas, Acid activation of a palygorskite with HCl: development of physico-chemical, textural and surface properties, Applied Clay Science 10 (1995) 247–258.
[21] J. Šesták, Thermal Analysis. Part D. Thermophysical Properties of Solids, their Measurements and Theoretical Thermal Analysis, 1984.
[22] Z. Rivlin, J. Baram, Numerical simulation of cluster growth during the transient nucleation period in melt-spinning, Materials Science and Engineering: A 173 (1993) 395–400.
[23] K.C. Russell, Nucleation in solids: the induction and steady state effects, Advances in Colloid and Interface Science 13 (1980) 205–318.
[24] A.M. Shams El Din, M.E. El Dahshan, A.M. Taj El Din, Dissolution of copper and copper–nickel alloys in aerated dilute HCl solutions, Desalination 130 (2000) 89–97.
[25] D. Panias, Taxiarchou, I. Paspaliaris, A. Kontopoulos, Mechanisms of dissolution of iron oxides in aqueous oxalic acid solutions, Hydrometallurgy 42 (1996) 257–265.
[26] D. Panias, M. Taxiarchou, I. Douni, I. Paspaliaris, A. Kontopoulos, Dissolution of hematite in acidic oxalate solutions: the effect of ferrous ions addition, Hydrometallurgy 43 (1996) 219–230.
[27] A.G. Kumbhar, K. Kishore, G. Venkateswaran, V. Balaji, Dissolution of Ce, Zr and La-containing magnetites and nickel ferrite in citric acid–EDTA–gallic acid formulation, Hydrometallurgy 68 (2003) 171–181.
[28] R.K. Iler, The Chemistry of Silica, Wiley, New York, 1979.
[29] S. Atalay, H.I. Adiguzel, F. Atalay, Infrared absorption study of Fe_2O_3–CaO–SiO_2 glass ceramics, Materials Science and Engineering A 304–306 (2001) 796–799.
[30] K. Shimoda, H. Miyamoto, M. Kikuchi, K. Kusaba, M. Okuno, Structural evolutions of $CaSiO_3$ and $CaMgSi_2O_6$ metasilicate glasses by static compression, Chemical Geology 222 (2005) 83–93.
[31] L. Peng, W. Qisui, L. Xi, Z. Chaocan, Investigation of the states of water and OH groups on the surface of silica, Colloids and Surfaces A: Physicochemical and Engineering Aspects 334 (2009) 112–115.
[32] S. Gunasekaran, G. Anbalagan, Spectroscopic study of phase transitions in natural calcite mineral, Spectrochimica Acta Part A: Molecular and Biomolecular Spectroscopy 69 (2008) 1246–1251.
[33] J. Nawrocki, The silanol group and its role in liquid chromatography, Journal of Chromatography A 779 (1997) 29–71.
[34] T.A. Guiton, C.G. Pantano, Infrared reflectance spectroscopy of porous silicas, Colloids and Surfaces A: Physicochemical and Engineering Aspects 74 (1993) 33–46.
[35] A.W. Musumeci, R.L. Frost, E.R. Waclawik, A spectroscopic study of the mineral paceite (calcium acetate), Spectrochimica Acta Part A: Molecular and Biomolecular Spectroscopy 67 (2007) 649–661.

[36] Y. Duan, J. Li, X. Yang, L. Hu, Z. Wang, Y. Liu, C. Wang, Kinetic analysis on the non-isothermal dehydration by integral master-plots method and TG–FTIR study of zinc acetate dihydrate, Journal of Analytical and Applied Pyrolysis 83 (2008) 1–6.
[37] S.S. Jewur, J.C. Kuriacose, Studies on the thermal decomposition of ferric acetate, Thermochimica Acta 19 (1977) 195–200.
[38] T. Arii, Y. Masuda, Thermal decomposition of calcium copper acetate hexahydrate by simultaneous measurement of controlled-rate thermogravimetry and mass spectrometry (CRTG–MS), Thermochimica Acta 342 (1999) 139–146.
[39] M.A. Mohamed, S.A. Halawy, M.M. Ebrahim, Non-isothermal decomposition of nickel acetate tetrahydrate, Journal of Analytical and Applied Pyrolysis 27 (1993) 109–110.